Landslide Susceptibility Assessment Using GIS and RS In the Havran River Basin (Balikesir-TURKEY)

Hasan Ozdemir, Huseyin Turoglu

Geography Department, Istanbul University, Ordu Cad. No: 196, 34459, Laleli, Istanbul, Turkey
E-mail: ozdemirh@istanbul.edu.tr, turogluh@istanbul.edu.tr

1. Abstract

In this study we assess landslide susceptibility of Havran river basin using Geographical Information Systems (GIS), Remote Sensing (RS) data and the statistical index method. Landslide locations were interpreted from topographic maps and verified with field observations. The collected data was combined in a spatial database using GIS and RS. Lineament, NDVI and Land use/cover data of the basin were extracted from Landsat ETM+ and Spot XS satellite images. Other contributing factors of elevation, slope, aspect, curvature, lithology, distance to roads, rainfall and soil data of the basin were also included. A GIS-based assessment process was constructed using these eleven factors and a statistical index method was used to produce a map of susceptibility. The results of the analysis were verified using the original landslide location data. The comparison between the predicted result and the actual distribution of landslides showed a high consistency.

2. Introduction

In more than 10 years different methods and techniques for evaluating landslide occurrence have been developed and proposed worldwide (Hansen, 1984; Varnes, 1984; Hutchinson, 1995; Crozier, 1995). These methods include inventory mapping (direct approach) and a set of indirect, quantitative methods, namely the knowledge-based (index), statistical (data-driven) and deterministic approaches (Carrara et al., 1998). Quantitative methods rely on observed relationships between controlling factors and landslides (Guzzetti et al. 1999). Statistical analysis in quantitative methods are used to obtain predictions of the mass-movement from a number of parameter maps (Yin and Yan, 1988; Gupta and Joshi, 1990; Lee et al., 2002; Ayalew et al., 2004; Carrara et al., 1991; Chung and Fabbri, 1999). They can be categorized into two subgroups according to their data analysis methods: bivariate and multivariate (Soeters and Van Westen, 1996). The bivariate models consider each individual thematic map in terms of landslide distribution and can be easily implemented in GIS (van Westen 1997). Mapping past and recent slope movements, together with the identification and mapping of the conditioning or preparatory factors of slope instability, are key components for predicting future landslides (Carrara et al., 1998). Generally, the purpose of landslide susceptibility mapping is to highlight the regional distribution of potentially unstable slopes based on a detailed study of the contributing factors (Ayalew et al., 2004).

Since susceptibility mapping involves the handling and interpreting of a large amount of data, the use of GIS is very important. One advantage of assessing landslide susceptibility using GIS is the speed at which calculation can be performed. Additionally, complex techniques requiring a large number of map crossings and table calculations are feasible. Furthermore, RS has an important role in assessing the susceptibility of landslides. This study reveals that remote sensing data are mostly used in preparation of some predisposing factors for the assessment. So far, RS data have played a minor role in landslide investigations because of their limited resolution and the small size of landslide. Using topographical maps and field surveys, 84 landslides were determined in the study area. In order to assess the susceptibility in the area we used the statistical index method (van Westen, 1997) to qualitatively define the weight values. However, many different methods exist for the calculation of weight values.

3. Study Area

The Havran river basin is situated between the coordinates 494530 – 530806 Y and 4365088 - 4395802 X coordinate (UTM, ED 50, Zone 35 N) in the western part of the Balikesir district, western Turkey. With a perimeter of 138.8 km and covering an area of about 570 km^2 (Fig. 1), the elevation of the basin changes between 0-1290 m.

In the area, a total of 84 landslides have been determined from topographic maps and field surveys (Table 1, Fig. 1). All the landslides were classified into five types which are rotational slides, rock fall, debris flow, earth flow and topple (Table 1, Fig. 2). Some statistical properties of landslides are given in Table 1. Rotational movements represent 42% of the total landslides. They have the highest area with 73.3% of the total landslide area. Rock falls represent 23.8% of the total movements and cover a total area of 21.1%. Debris flow, earth flow and topple have less area compared the first two types (Table 1).

Geologically, the study area consists of four main types of lithological units: metamorphic basement rocks of Paleo-zoic-Mesozoic (schists, metagrabbros, amphibolities, phyllites, recrystallized limestone; granitic plutons of Upper Oligosen-Lower Miocene; Ayvacık volcanics of Lower- Middle Miocene (intermediate lavas and pyroclastic rocks) and alluvium of Quaternary (pebble, sand, silt and clay).

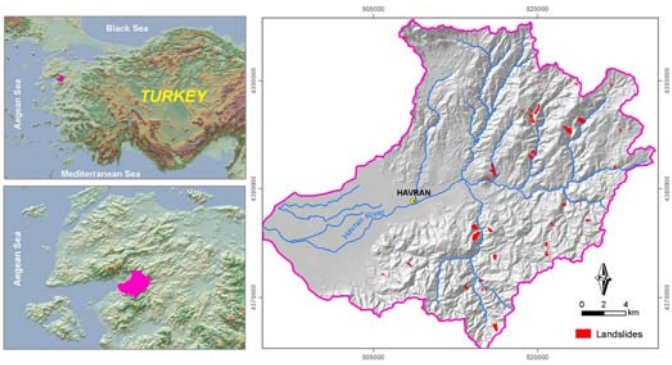


Fig.1. Location of study area and spatial distribution of landslides.

Table 1 Some statistical properties of landslides.

Types	No	% of Total	Area Min. (m^2)	Area Max. (m^2)	Total Area (m^2)	% of Total Area
Rotational Slide	42	50	590	338519	2979800	73.3
Rock Fall	20	23.8	1567	262427	857093	21.1
Debris Flow	15	17.8	641	45677	183800	4.6
Earth Flow	4	4.8	4350	10985	28671	0.7
Topple	3	3.6	3301	3887	10560	0.3
Total	84	100	590	338519	4059924	100

According to Zezere (2002), different types of landslides have neither the same magnitude nor equal damaging potential. Furthermore, technical strategies to mitigate land sliding also depend on landslide typology. These are additional reasons to discriminate between different types of slope movements when assessing landslide susceptibility and hazard. However in this case, for the statistical analysis, landslide typology has not been mentioned due to the low number of landslides.

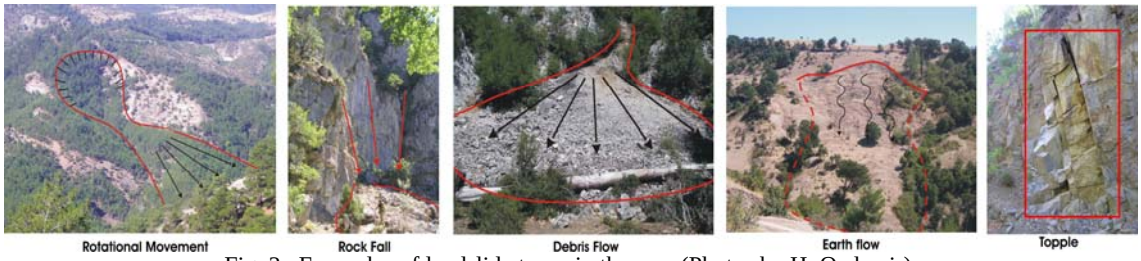


Fig. 2. Examples of landslide types in the area (Photos by H. Ozdemir).

4. Data Collection and Database Construction

The construction of a cartographic database, comprising of the eleven maps used for landslide susceptibility assessment, was based on three different tasks: 1) digitizing, editing and analyzing of analog maps, 2) visual interpretation and classification of the satellite images, and 3) detailed field surveying (Fig. 3).

Topographical maps scaled 1:25000 was registered in the UTM projection plane (ED 50 Zone 35 N) and digitized in 10 m contour interval. The digital elevation model (DEM) was created from 10 m contour lines by a linear interpolation. Some layers were produced using the DEM, including slope angle, aspect and surface curvature on the basis of a moving 3x3 cell window. These criteria are proven to be predisposing factors for landslide activity. A pixel size of 10 m (100 m^2) was adapted to the DEM layer as well as the other parameters presented in Table 2. Visual interpretation based on filtered image products, band ratio and supervised classification was the main techniques applied in the analysis of the RS data.

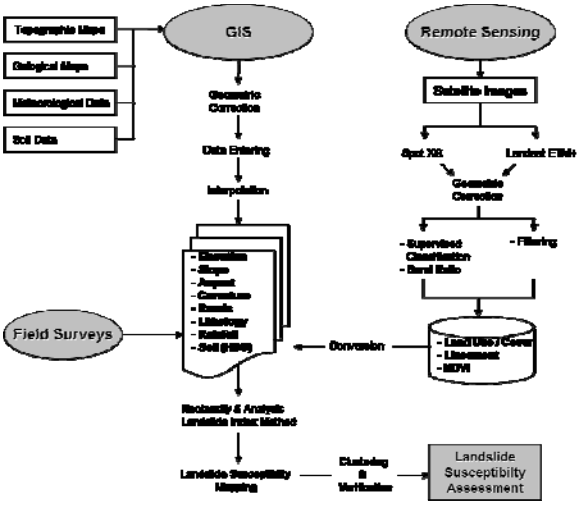


Fig. 3. Flowchart of general methodology.

Table 2 Attribute data of parameters for susceptibility.

ID	Parameter Subclasses	∑Pix	Pix. No in Landslides	Density in Subclass	Index Method W_i
	Elevation				
1	0-250	2111377	4617	0.00219	-1.19018
2	250-500	1682408	22299	0.01325	0.60992
3	500-750	1623388	11803	0.00727	0.00968
4	750-1000	259327	2141	0.00826	0.13734
5	1000-1290	27244	243	0.00892	0.21421
	Curvature				
1	-0.39- (-0.01) Concave	704698	7386	0.01048	0.37539
2	(-0.01)-0.006 Strait	3759078	22823	0.00607	-0.17072
3	0.006-0.34 Convex	1239967	10894	0.00879	0.19953
	Lithology				
1	Tufe	15723	15	0.00095	-2.02537
2	Alluvium	989814	20	0.00002	-5.88610
3	Permien Olistolite	9647	0	0	
4	Granitic Pluton	387308	874	0.00226	-1.15872
5	Metagrovacs	626052	384	0.00061	-2.46838
6	Andesite and Tufe	2233032	24172	0.01082	0.40732
7	Alluvium Old	11443	0	0	
8	Neogen Sediment	367997	880	0.00239	-1.10279
9	Epimetamophise	149456	262	0.00175	-1.41447
10	Hornfles, Granotit	24343	0	0	
11	Limestone	224558	8463	0.03769	1.65531
12	Conglomerate	113447	1596	0.01407	0.66996
13	Dasite and Riolite	495875	3950	0.00797	0.10160
14	Poligenic Aglomerate	55397	487	0.00879	0.19953
	Slope (°)				
1	0-2	1242894	471	0.00038	-2.94167
2	2-15	1900495	12825	0.00675	-0.06454
3	15-25	1742484	13876	0.00796	0.10035
4	25-45	812712	12970	0.01596	0.79600
5	45-<	5158	961	0.18631	3.25333
	Aspect				
1	Flat (-1)	378238	237	0.00063	-2.43612
2	N (337.5-22.5)	614889	4916	0.00799	0.10411
3	NE (22.5-67.5)	439101	5783	0.01317	0.60386
4	E (67.5-112.5)	492395	7713	0.01566	0.77703
5	SE (112.5-157.5)	620659	8238	0.01327	0.61142
6	S (157.5-202.5)	578782	2913	0.00503	-0.35866
7	SW (202.5-247.5)	715914	2311	0.00323	-0.80160
8	W (247.5-292.5)	921288	3931	0.00427	-0.52247
9	NW (292.5-337.5)	942478	5061	0.00537	-0.29325
	Land Use/Cover				
1	Forest	2027098	25667	0.01267	0.56516
2	Iron mine	3392	0	0	
3	Agricultural Area	280656	21	0.00007	-4.63334
4	Maquis Area	793343	7124	0.00898	0.22092
5	Grass Area	243237	931	0.00383	-0.63122
6	Olive agriculture	852366	2344	0.00275	-0.96248
7	Settlement- Barren land	1499762	5006	0.00334	-0.76811
	NDVI				
1	-0.56-0.067	1471161	4478	0.00304	-0.86222
2	0.067-0.28	2001613	10931	0.00546	-0.27663
3	0.28-0.79	2228462	25694	0.01153	0.47087
	Rainfall				
1	581-704	1571100	0	0	
2	7704-837	1550400	15147	0.00977	0.30524
3	837-963	1320700	13806	0.01045	0.37252
4	963-1133	1118200	11288	0.01009	0.33746
5	1133-1429	142900	862	0.00603	-0.17733
	Distance to Lineament				
1	500	2546719	21474	0.00843	0.15772
2	1000	1493490	11770	0.00788	0.09025
3	1500	704122	4779	0.00679	-0.05863
4	2000	333655	1141	0.00342	-0.74444
5	2000<	626106	1939	0.00310	-0.84268
	Distance to Roads				
1	50	1375704	7910	0.00575	-0.22488
2	100	1114109	6653	0.00597	-0.18733
3	150	867875	5779	0.00666	-0.07796
4	200	657163	4944	0.00752	0.04349
5	200<	1689241	15817	0.00936	0.26236
	Soils (HSG)				
1	A	25068	0	0	
2	B	229059	0	0	
3	C	846496	86	0.00010	-4.27667
4	D	4602840	41017	0.00891	0.21309

Finally, some predisposing factors were prepared for susceptibility assessment using RS techniques.

Slope angle, aspect of slope and profile curvature data have been derived from DEM. The slope angle layer was classified into 5 classes in order to more accurately represent site conditions. The aspect layer represents the angle between the the Geographic North and horizontal plain for a certain point and is classified by 8 major orientations (N, NE, E, SE, S, SW, W, NW) with the addition of flat areas. Profile curvature is divided by concave, convex and flat topographic surfaces. Lithology was obtained from the geological map of the region (1:100000). The geological boundaries of the 14 lithological units were verified and validated through fieldworks (Table 2). Road maps were obtained from topographical maps of the basin. In this study, a 50 m buffer (25+25) was applied to all types of roads based on field work observation. Land use/cover was obtained from Spot XS (2005) satellite images in conjunction with supervised classification and field works. Land use/cover was classified in 7 classes. 250 m interval was used in elevation range due to tectonic evidences. Soil data was obtained from GDRS (General Director of Rural Services) in 1:25000 scales. Based on their hydrologic properties for water conditions and infiltration capacity, four units were classified. NDVI (Normalized Difference Vegetation Index) data was obtained from Spot XS satellite images and described in three subclasses which are dense vegetation, sparse vegetation and non vegetated areas. A lineament map was created using 4, 5, 7 bands of Landsat ETM+ dated 2000 (Akhir et al., 1997; Voldai, 1995; Suzen et al., 1998). A Sobel directional filter was applied to the bands and five classes were determined. Rainfall data was obtained from meteorological stations located near the basin. Using interpolation techniques an annual rainfall map was created for the entire basin in five classes (Table 2).

5. Landslide Susceptibility Assessment and Validation

The applied statistical index method for the susceptibility assessment is based on a frequency analysis.

This method simply defines the importance of a parameter subclass on landslide occurrence according to the spatial distribution of pixel of the considered parameter in relation to the landslide pixels. A standardization of the density values can be obtained by relating them to the overall density in the entire area. In this study the landslide density for each class is divided by the landslide density in for the entire map.

The natural logarithm is used to give negative weights when the landslide density is lower than normal and positive when it is higher than normal (Van Wasten, 1997). By combining eleven maps of weight-values, a

susceptibility map was created. According to the description, W_i is expressed as in following equation:

$$Wi = \ln \frac{Densclas}{Densmap} = \ln \left(\frac{\frac{Npix(S_i)}{Npix(N_i)}}{\frac{\sum Npix(S_i)}{\sum Npix(N_i)}} \right)$$

Where,
W_i = the weight given to a certain parameter class (e.g. lithology, or a slope class)
Densclas = the landslide density within the parameter class.
Densmap = the landslide density within the entire map.
$Npix(S_i)$ = number of pixels, which contain landslides, in a certain parameter class.
$Noix(N_i)$ = total number of pixels in a certain parameter class.
W_i values were calculated according to the pixel values tabulated in Table 2. The result of the calculation is given in Fig. 4a as non-classified. Final values of pixels are changingbetween -23.46 (low susceptibility) to 8.71 (high susceptibility). Classification of the final map into different susceptibility classes is very difficult. For this purpose, some authors use different kinds of techniques such as expert opinion, standard deviation, natural break, quantiles, equal interval etc. In this study, we considered cluster analysis based on iterative minimum distance of each pixel in five classes (Forgy, 1965) using SAGA GIS software (Fig. 4b).

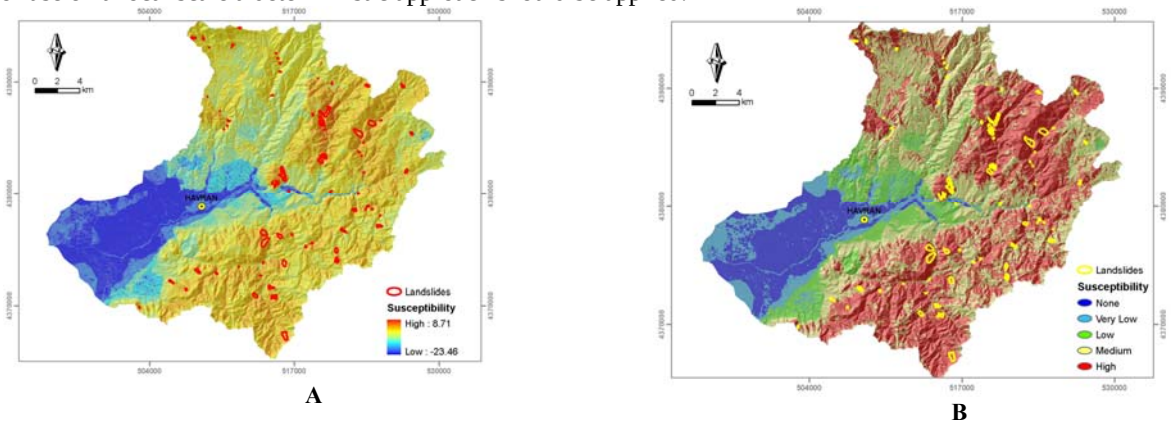
As is shown in Fig. 4b the five categories correspond to five relative scales of landslide susceptibility, namely none (or extremely low), very low, low, medium and high.

In order to validate the results of the susceptibility assessment, the same landslide data set was used. Interpretation of Fig. 5a and b allow the identification of the following susceptibility classes:

Ⅰ) The high susceptibility class includes 2 114 866 pixels (the largest susceptibility values that cover 37.22 % of study area) and 81.15% of the area of landslides;
Ⅱ) The medium susceptibility class includes 1 8 82 317 pixels (33.13% of the study area) and includes 17.94% of landslides.
Ⅲ) The low susceptibility class includes 636 979 pixels (11.21% of the study area) and includes 0.89% of landslides.
Ⅳ) The very low susceptibility class includes 438 928 pixels (7.72% of the study area) and includes 0.03% of landslides.
Ⅴ) The extremely low susceptibility class includes 609 147 pixels (10.72% of the study area) with no landslides located in this area (0.00%).

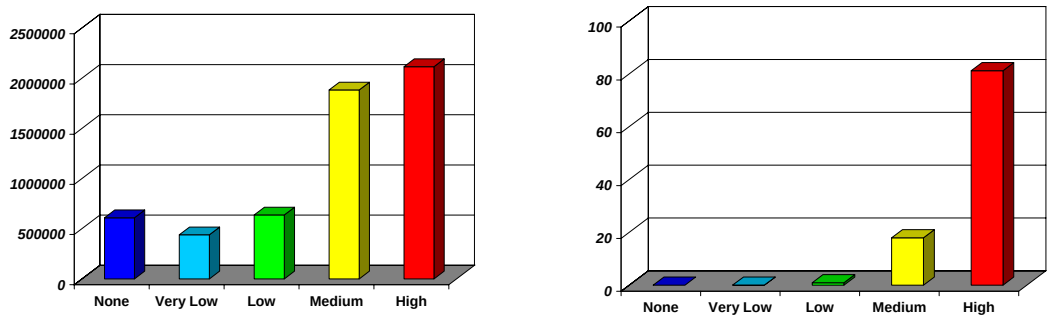
6. Conclusion

The spatial distribution of landslides is a result of the interaction of many parameters. To create an accurate susceptibility map, proper parameters must be used. In this study eleven parameters namely, elevation, curvature, lithology, slope, aspect, land use/cover, NDVI, rainfall, lineament, roads and soil were considered. To create some parameters RS techniques were used. A method called statistical index method was used to extract the weight of each parameter. This method pointed out the importance of lithology and slope parameters above others, on landslide occurrence. The results of the entire analysis and evaluation allowed us to divide the study area into five zones of susceptibility, namely none or extremely low (10.72%), very low (7.72%), low (11.21%), medium (33.13%) and high (37.22%). Validation of the results, using same landslide data set, showed that the high susceptible zone includes 81.15% of landslide areas. All these studies have been done on a basin scale as it allows us to determine general probable landslide areas. In order to obtain a more precise result for use on a local scale a deterministic approach should be applied.



A B

Fig. 4. (A) Non-classified landslide susceptibility map of Havran River basin (B) Landslide susceptibility map of Havran River basin, classified according to minimum distance clustering method.



A **B**

Fig. 5. (A) Distribution of susceptibility classes in susceptibility classes. (B) Percentage of landslide distribution

7. Acknowledgement

This work was supported by the Research Found of Istanbul University. Project number: T-583/17032005. Authors thank to Deanne Bird for her help.

8. References

Akhir, J.M., Abdullah, I., 1997. Geological Application of Landsat TM Imagery: Mapping and Analysis of Lineament in NW Peninsula Malaysia (www.gisdevelopment.net).

Ayalew, L., Yamagishi, H., Ugawa, N., 2004. Landslide susceptibility mapping using GIS-based weighted linear combination, the case in Tsugawa area of Agano River, Niigata Prefecture, Japan. Landslides 1, 73-81.

Carrara, A., Cardinali, M., Detti, R., Guzzetti, F., Pasqui, V., Reichenbach, P., 1991. GIS techniques and statistical models in evaluating landslide hazard. Earth Surface Processes and Landforms 16, 427-445.

Carrara, A., Guzzetti, F., Cardinali, M., Reichenbach, P., 1998. Current limitations in modeling landslide hazard. In: Buccianti, A., Nardi, G., Potenza, R. (Eds.), Proceedings of IAMG'98, pp. 195-203.

Chung, C.-J.F., Fabbri, A.G., 1999. Probabilistic prediction models for landslide hazard mapping. Photo. Eng. Remote Sens 65, PP. 1389-1399.

Crozier, M.J., 1995. Landslide hazard assessment, theme report. In: Bell (Ed.), Landslides, Proceedings of the 6th International Symposium on Landslides, Balkema, Rotterdam, pp. 1843-1848.

Forgy, E.W., 1965. Cluster analysis of multivariate data: efficiency vs interpretability of classifications. Biometrics 21, 768-769.

Gupta, R.P., Joshi, B.C., 1990. Landslide hazard zonation using the GIS approach-a case study from the Ramganga Catchment, Himalayas. Eng. Geol. 28, 119-131.

Guzzetti, F., Carrara, A., Cardinali, M., Reichenbach, P., 1999. Landslide hazard evaluation: a review of current techniques and their application in a multi-scale study, Central Italy. Geomorphology 31, 181-216.

Hansen, A., 1984. Landslide hazard analysis. In: Brunsden, D., Prior, D.B. (Eds.), Slope Instability. John Wiley and Sons, Chichester, pp. 523-602.

Hutchinson, J.N., 1995. Landslide hazard assessment, keynote paper. In: Bell (Ed.), Landslides, Proceedings of the 6th International Symposium on Landslides. Balkema, Rotterdam, pp. 1805-1841.

Lee, S., Choi, J., Min, K., 2002. Landslide susceptibility analysis and verification using the Bayesian probability model. Environ Geol. 43, 120-131.

Soeters, R., van Westen, C.J., 1996. Slope instability recognition, analysis, and zonation. In: Turner, A.K., Schuster, R.L. (Eds.), Landslides: investigation and mitigation. Transport Res. Board Spec. Rep. 247, pp. 129-177.

Suzen, M.L., Toprak, V., 1998. Filtering of Satellite Images in Geological Lineament Analysis: An Application to Fault Zone in Central Turkey. International Journal of Remote Sensing 19, 1101-1114.

Van Westen, C.J., 1997. Statistical landslide hazard analysis. In: Application guide, ILWIS 2.1 for Windows. ITC, Enschede, The Netherlands, pp. 73-84.

Varnes, D.J., 1984. Landslide hazard zonation: a review of principles and practice. UNESCO, Paris.

Voldati, T., 1995. Multiple-sources Remotely Sensed data for Lithological and Structural Mapping. ITC Journal 2, 95-113.

Yin, K.L., Yan, T.Z., 1988. Statistical prediction model for slope instability of metamorphosed rocks. In: Bonnard, C. (Ed.), Proc. 5th Int. Sym. on Landslides, Lausanne. Balkema, Rotterdam, pp. 1269-1272.

Zezere, J.L., Reis, E., Garcia, R., Olieira, S., Rodrigues, M.L., Vieira, G., Ferreira, A.B., 2004. Integration of spatial and temporal data for the definition of different landslide hazard scenarios in the area north of Lisbon (Portugal). Natural Hazards and Earth System Science 4, 133-146.